

***k*-Relevance Vectors for Pattern Classification**

Peyman Hosseinzadeh Kassani^{1,*}, Sara Hosseinzadeh Kassani²

¹Department of Biomedical Engineering, Tulane University, New Orleans, LA, USA

²Department of Computer Science, University of Saskatchewan, Saskatchewan, Canada

Highlights

- New concept of similarity; relevancy beside nearness.
- Proposed a highly sparse method with good classification accuracy.
- Proposed a new parameter that helps to improve the final accuracy.
- Validated the proposed model on several datasets.

Abstract:

This study combines two different learning paradigms, *k*-nearest neighbor (*k*-NN) rule, as memory-based learning paradigm and relevance vector machines (RVM), as statistical learning paradigm. This combination is performed in kernel space and is called *k*-relevance vector (*k*-RV). The purpose is to improve the performance of *k*-NN rule. The proposed model significantly prunes irrelevant attributes. We also introduced a new parameter, responsible for early stopping of iterations in RVM. We show that the new parameter improves the classification accuracy of *k*-RV. Intensive experiments are conducted on several classification datasets from University of California Irvine (UCI) repository and two real datasets from computer vision domain. The performance of *k*-RV is highly competitive compared to a few state-of-the-arts in terms of classification accuracy.

Keywords: Nearest neighbor rule, Relevance vector machine, Sparsity, Sparse Bayesian learning

1- Introduction

Pattern classification is one of the major components of intelligent systems and has numerous applications in several research areas [1-7]. The purpose is to assign unseen / test data to either the positive or negative category [8]. Support vector machines (SVM) [9], decision trees [10], *k*-nearest neighbor (*k*-NN) rule [11], naïve Bayes [8] are among most popular classifiers. Among them, the simple yet powerful *k*-NN rule is one of top ten known data mining algorithms [12] and has attained popularity since 1967 [11]. *k*-NN rule is an instance-based learning algorithm in which the prediction for a query instance is regionally calculated through nearest neighbors of that query instance. Nearness is known as similarity measurement and is usually calculated with Euclidean distance between the query instance and its neighbors. If number of neighbors, *k* is equal

to 1, the query data is assigned to the class of the nearest neighbor, i.e. the one has shortest Euclidean distance to the query instance. The complexity of k -NN rule is $O(Nl)$ where N is the total number of training data and l is the size of data columns. This complexity increases if the value of k increases. On the other hand, different values of k may alter the target value of the query instance, and hence, selecting a good value of k is a non-trivial task.

k -NN has been applied to several applications such as medical diagnosis [13-15], intrusion detection [16, 17], image classification [18-20], video multimedia classification and segmentation [5, 21, 22]. Regardless of the merits of k -NN rule, it has two problems in learning from data. First, k -NN uses distance metric to calculate similarities between instances. k -NN assumes all variables equally contribute to the learning procedure which may lead to poor prediction if some variables are redundant. Additionally, the main patterns in data are contained in just a few variables. In this sense, weight assignment may better increase the accuracy of the nearest neighbor rule [23]. Second, the presence of noise in data may jeopardize the k -NN performance during calculating the similarity between instances [23]. For this problem, one can modify the distance measurement. The importance of each attribute can be evaluated via weight assignment to each attribute. This method is known as attribute weighting method [23-28].

Tutz and Ramzan [28] used w -NN for imputation of missing data. The careful selection of distances using weights helped discover more information of the missing values and outperformed competing nearest neighbor methods. The main idea of study in [23] is to refine the distance metric of k -NN based on the Minkowski distance in order to include only a subset of relevant variables. Experimental results on low- and high-dimensional datasets demonstrate the importance of these modifications. Takeuchi et.al propose an attribute selection and weighting method [25] for improvement of k -NN classifier. With a novel attribute weighting algorithm, the correct target neighbor is obtained, and nearest neighbors are updated through a sequential quadratic programming. This approach gained better performance than traditional k -NN.

In this study, using a simple yet versatile algorithm, the proposed k -RV rule may less suffer from the mentioned problems. We use sparsity to prune irrelevant and noisy attributes [29-31]. We borrow the idea of sparse Bayesian learning in RVM and combine it with k -NN. In [32], two drawbacks of extreme learning machine (ELM) [33], i.e. 1) suffering from overfitting problem and 2) sensitivity of the accuracy of ELM to the number of hidden neurons are resolved by relevance

vector machine (RVM) [31] as sparse Bayesian learning (SBL) approach. During the learning process, several redundant hidden neurons of ELM are detected and pruned.

Study in [34], also reduces the number of hidden neurons of multivariate polynomial (MP) and reduced polynomial (RP) [35] with the sparsity approach in RVM. The sparsed methods, i.e. sparse Bayesian RP (SBRP) and sparse Bayesian MP (SBMP) have better classification accuracy (CA) than MP and RP examined on several datasets.

In a similar fashion to [32, 34] as the source of inspiration for our study, we also modify the distance metric in k -NN rule through sparse Bayesian learning method used in RVM. The learned sparsed weights obtained by RVM is served as the importance of each attribute for w -NN rule. The non-zero weights are fed into the distance metric of w -NN. And hence this builds up a sparsed w -NN rule, that we called k -relevance vector (k -RV).

Another study that can be also related to our research is a combination of RVM and k -NN for the improvement of RVM. Rismanchian and Rahimian [36] used nearest neighbor rule separately for each test instance to find the neighbors, and then RVM is performed on the neighbors of each test instance. This method is called localized RVM (LRVM) since it locally classifies each test instance with RVM. The purpose was to heal the RVM performance that suffers from the degeneracy of covariance function [37]. In contrast to [36] that uses k -NN to improve RVM, in our research we use sparsity approach in RVM to make a sparsed nearest neighbor rule, called k -RV.

The contributions and advantages of k -RV are as follows:

1. We link two different learning approaches, k -NN as a memory-based learner and SBL as a statistical method for feature selection. Our combination adds a novel concept of similarity measurement into k -NN, we call k -relevancy, i.e. considering relevancy beside nearness.
2. We introduce a new parameter for early stopping of iterations in RVM. If query instance is far away from the RVs, then RVM may have poor prediction for that query instance [37]. We abort iteration in RVM if the change of α (The variable α is responsible for pruning train data) between current iteration i and previous iteration $i-1$ is smaller than a default value. We show that the performance of k -RV is further improved through tuning this parameter.

3. Intensive experiments on a generated toy data and two real-world data chosen from computer vision domain validate the reliability of k -RV comparing with several counterparts.

The remainder of this paper is organized as follows: Section two covers the related works, motivation and contributions. Section three discusses k -NN rule and RVM as preliminaries. Section four expresses the proposed k -RV rule. Some theoretical points are explained in discussion section. Section six examines experiments conducted on several UCI datasets and two real databases chosen from computer vision domain. Last section pays attention to remarks and concludes this paper.

2. Preliminaries

2.1. k -NN and w -NN rules

Assume $(\mathbf{x}_1, \mathbf{t}_1), (\mathbf{x}_2, \mathbf{t}_2), \dots, (\mathbf{x}_N, \mathbf{t}_N)$ be N data points in which \mathbf{x}_i is the training input and with D dimensions and \mathbf{t}_i is the target value. To find the k nearest neighbors of the query instance \mathbf{z} , the Euclidean distance is performed as follows:

$$Dist_{k-NN}(\mathbf{x}, \mathbf{z}) = \sqrt{\sum_{i=1}^D (x_i - z_i)^2} \quad (1)$$

where \mathbf{x} and \mathbf{z} are respectively train and test vectors. The pairwise distance comparison between the query instance \mathbf{z} and each of N training instances \mathbf{x} is computed. The k number of training instances with shortest distance to \mathbf{z} are nearest neighbors.

Moreover, the importance of each attribute can be evaluated through weight assignment into Eq. (1). This method is known as weighting nearest neighbor rule or w -NN. The new equation for w -NN is as follows:

$$Dist_{w-NN}(\mathbf{x}, \mathbf{z}) = \sqrt{\sum_{i=1}^D w_i (x_i - z_i)^2} \quad (2)$$

Weight w_i for each attribute may change the order of neighbors and may improve the accuracy of k -NN.

2.2. Relevance vector machine

Sparse Bayesian learning (SBL) and in particular relevance vector machine (RVM) [38] is a probabilistic formulation to support vector machine (SVM) [39]. To estimate the target vector $\mathbf{t} \in \mathbb{R}^{1 \times N}$ in kernel space, we suppose $\mathbf{t} = \mathbf{w}^T \mathbf{H}$ where $\mathbf{w} \in \mathbb{R}^{(N+1) \times 1}$ is weight vector and $\mathbf{H} \in \mathbb{R}^{(N+1) \times N}$ is design matrix with N training instances. For classification task, each training instance $\mathbf{x} \in \mathbb{R}^{N \times l}$ with l dimension is supposed to be drawn from an independent Bernoulli random variable with probability $p(\mathbf{t}|\mathbf{x})$ where $\mathbf{t} \in \mathbb{R}^{1 \times N}$ is a target vector. Additionally, one can choose posterior probability $p(\mathbf{w}, \boldsymbol{\alpha}|\mathbf{t})$ as objective function with $\boldsymbol{\alpha} \in \mathbb{R}^{(N+1) \times 1}$ as hyperparameter vector. Showing this for N training instances with Bernoulli likelihood,

$$p(\mathbf{t}|\mathbf{w}) = \prod_{i=1}^N \sigma\{g(\mathbf{h}_i; \mathbf{w})\}^{t_i} [1 - \sigma\{g(\mathbf{h}_i; \mathbf{w})\}]^{1-t_i} \quad (3)$$

where \mathbf{k}_i , g , and σ are respectively i^{th} column vector of the kernel matrix \mathbf{H} , the network output and the nonlinear Sigmoid function. A closed form solution cannot be achieved since Sigmoid is a nonlinear function. Hence, according to [38], iterative Mackay procedure [40] is necessary to get the marginal likelihood.

To solve the posterior probability $p(\mathbf{w}, \boldsymbol{\alpha}|\mathbf{t})$ in an easy way, its decomposed part, i.e. marginal likelihood $p(\mathbf{w}|\mathbf{t}, \boldsymbol{\alpha})$ is optimized:

$$p(\mathbf{w}|\mathbf{t}, \boldsymbol{\alpha}) \propto p(\mathbf{t}|\mathbf{w})p(\mathbf{w}|\boldsymbol{\alpha}) \quad (4)$$

Let $p(w_i|\alpha_i) \approx N(0, \alpha_i^{-1})$, and then three subsequent techniques, namely marginalization, Laplace approximation, and Iterative Regularized Least Square (IRLS) are used to calculate $\hat{\mathbf{w}} \in \mathbb{R}^{(N+1) \times 1}$ and $\boldsymbol{\Sigma} \in \mathbb{R}^{(N+1) \times (N+1)}$ as follows:

$$\hat{\mathbf{w}} = \boldsymbol{\Sigma} \mathbf{H}^T \mathbf{B} \mathbf{t} \quad (5)$$

$$\boldsymbol{\Sigma} = (\mathbf{H}^T \mathbf{B} \mathbf{H} + \mathbf{A})^{-1} \quad (6)$$

where $\hat{\mathbf{w}} \in \mathbb{R}^{(N+1) \times 1}$ is posterior mode of \mathbf{w} and $\mathbf{A} = \text{diag}(\boldsymbol{\alpha})$ and \mathbf{B} is a diagonal matrix with diagonal elements $(\beta_1, \beta_2, \dots, \beta_N)$ where $\beta = \sigma\{t(\mathbf{x}_n)\}[1 - \sigma\{t(\mathbf{x}_n)\}]$. Once $\boldsymbol{\Sigma}$ and $\hat{\mathbf{w}}$ are initialized, the hyper-parameters α_i are updated as follows,

$$\alpha_i^{\text{new}} = \frac{1 - \alpha_i \Sigma_{ii}}{\hat{w}_i^2} \quad (7)$$

where \hat{w}_i , and Σ_{ii} are the i^{th} posterior weight and the i^{th} diagonal element of $\boldsymbol{\Sigma}$ computed with Eq. (5) and Eq. (6). This is an iterative algorithm and the parameters in Eq. (5), (6), and (7) should be

repeated till to reach a stopping criterion. Since α has inverse relationship to w , many α 's tend to infinity and hence the corresponding w_i 's tend to zero. Simply, pruning elements from vectors \mathbf{w} , α and the corresponding basis vectors from \mathbf{H} yields sparsity.

3. Proposed k -RV rule

3.1 Overview

The proposed k -RV is tailored to three main steps, namely, data kernelization with Gaussian and Polynomial kernels, kernel data sparsification with RVM, and final classification with sparsed weights. Fig. 1 shows the flowchart of the proposed k -RV.

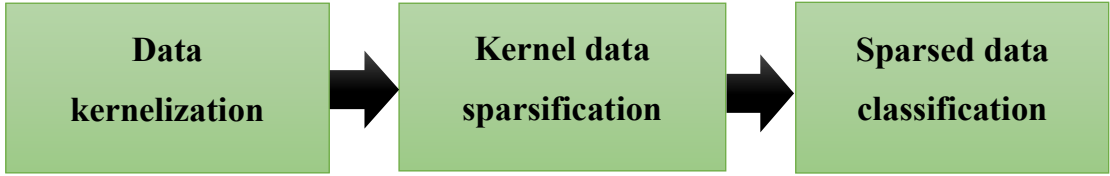


Fig. 1. Flowchart of the proposed method

These three stages build up our proposed k -RV.

3.2. k -RV: combination of k -NN and RVM

After kernelizing and pruning kernel matrix \mathbf{H} with the sparsity approach in RVM, the sparsed weights \mathbf{w}^{sp} and corresponding sparsed kernel matrix \mathbf{H}^{sp} are fed into the distance metric in nearest neighbor rule. The distance metric in k -RV is modified as follows:

$$Dist_{k-RV}(\mathbf{h}^{sp}, \mathbf{z}^{sp}) = \sqrt{\sum_{i=1}^D w_i^{sp} (h_i^{sp} - z_i^{sp})^2} \quad (8)$$

where z_i^{sp} is the i -th sparsed test instance. The class assignment for the test instance is performed with majority voting technique. The flowchart of the proposed k -RV is shown as follows:

Algorithm 1. k -RV

Initialization and kernelization

1. Initialize \mathbf{w} , α , Σ , and length of Gaussian kernel and the number of neighbors k .
2. Expand the input training matrix \mathbf{X} to the feature matrix \mathbf{H} with Gaussian or Polynomial kernel function.

Sparsification**While** $\Delta\alpha > 0.1$

3. Find α through $\alpha_i^{new} = \frac{1-\alpha_i\Sigma_{ii}}{\hat{w}_i^2}$ with initialized \mathbf{w} and Σ .
4. $\hat{\mathbf{w}} = \Sigma\mathbf{H}^T\mathbf{B}\mathbf{t}$, $\Sigma = (\mathbf{H}^T\mathbf{B}\mathbf{H} + \mathbf{A})^{-1}$, $\alpha_i^{new} = \frac{1-\alpha_i\Sigma_{ii}}{\hat{w}_i^2}$

End While**Classification****For** $i = 1$: number of test instances

5. Calculate $Dist_{k-RV}(\mathbf{h}^{sp}, \mathbf{z}^{sp}) = \sqrt{\sum_{i=1}^D w_i^{sp} (h_i^{sp} - z_i^{sp})^2}$
6. Assign the target value for every test instance using majority voting and RVs

End For.

4. Experiments

4.1. Datasets and Setup

Twenty datasets are selected from UCI data repository. To select these datasets, we care about both small size and large size in terms of the number of instances, binary and multi-class classification tasks. The descriptions of datasets are listed in the Table 1.

Table 1. Descriptions of datasets*

#	Dataset	# instances	# attributes (R/I/N)*	# Classes
Binary class problems				
1	Wbcd	683	9 (0/9/0)	2
2	Australia	690	33 (32/1/0)	2
3	Heart	270	13 (1/12/0)	2
4	Teaching	151	6 (0/6/0)	2
5	Ionosphere	351	33 (32/1/0)	2
6	Pima	768	8 (8/0/0)	2
7	Bupa	345	6 (1/5/0)	2
8	Shuttle	253	7 (0/7/0)	2
9	Parkinson	195	23 (23/0/0)	2
10	Titanic	2201	3(3/0/0)	2
11	Sonar	208	60 (60/0/0)	2
Multi-class problems				
12	Iris	150	4 (4/0/0)	3
13	Wine	178	13 (13/0/0)	3
14	Balance	625	4 (4/0/0)	3
15	Vehicle	846	18 (0/18/0)	4
16	Nursery	12960	8 (8/0/0)	5

17	Zoo	101	16 (0/0/16)	7
18	Segment	2310	19 (19/0/0)	7
19	Ecoli	336	7 (7/0/0)	8
20	Pendigit	10992	16 (0/16/0)	10

* R: real, I: integer, N: nominal

Some notes for the experimental setup:

1. The performance of the proposed k -RV is compared with ker-NN, RVM with Gaussian likelihood (RVM-Gauss), and RVM with Bernoulli likelihood (RVM-Bern).
2. For k -NN based learners, the value for k is in the range $\{1, 2, 3, \dots, 51\}$. To report the CA, we use the best value for k to predict the test labels. To find the best value for k , 10 runs of 10-fold cross validation is performed, and the average of CA is taken into consideration.
3. The new parameter $\Delta\alpha$ of k -RV is the difference between the α at current iteration with the α in the previous iteration. So, $\Delta\alpha$ is set to $\{10^{-6}, 10^{-5}, 10^{-4}, 10^{-3}, 10^{-2}, 10^{-1}, 1, 10\}$. Different $\Delta\alpha$ gives different number of RVs.
4. The width σ of Gaussian kernel $K(\mathbf{u}, \mathbf{v}) = \exp\left(\frac{\|\mathbf{u}-\mathbf{v}\|^2}{2\sigma^2}\right)$ for both ker-NN and k -RV is in the range of $\{0.05, 0.10, \dots, 1\}$. The order c of polynomial kernel $K(\mathbf{u}, \mathbf{v}) = (\mathbf{u} \cdot \mathbf{v} + 1)^c$ is set to $c = 2$ where \mathbf{u} and \mathbf{v} are two vectors in the input space.
5. The proposed model is implemented on a personal computer, with 32 GB RAM and with CPU 3.4 GHz, Intel Core i7. We use Matlab software to do experiments. The code is publicly available.

We also examine the learners in this article on two real world data. The first dataset is German Traffic Sign Recognition Benchmark (GTSRB) [4]. The GTSRB images are collected from the roads in Germany during daytime and nighttime and the images have high variations due to the illumination, sunlight exposure, occluded by the obstacles of the roadsides, and rotations. There are in total more than 50,000 images; 39,209 for training and 12,630 for test. The number of classes of signs are 43 with highly unbalanced frequencies. The size of signs in the images has high variations. The second dataset is MNIST handwritten digit recognition database [41] with 70,000 images; 60,000 for training and 10,000 for test, in 10 classes. The images are black and white. The images were centered by calculating the center of mass of the pixels and the size for every image is fixed at 28×28 . Fig. 2 displays instances for both MNIST and GTSRB data.



Fig. 2. Examples of real world datasets MNIST (in left) and GTSRB (in right)

To convert images to features, to be ready for learning purpose, we extract features with a histogram of Oriented Gradient (HOG) feature descriptor proposed by Dalal and Triggs at [42]. Cell size of HOG is set to 5×5 . Every four cells construct a block and we consider 50% overlapping between blocks. The number of bins is set to 8. With these values assigned to HOG parameters, the total feature size is 1568.

4.2. Results on UCI Data

Tables 2 and 3 tabulate the average CA of all learners including the proposed k -RV on 20 UCI datasets with Gaussian and polynomial kernels respectively.

Table 2. Average classification accuracy on 20 UCI data sets with Gaussian kernel.

Index	Model / Data set	ker-NN	k -RV	RVM-Gauss	RVM-Bern
1	WBCD	0.9267	0.9419	0.6964	0.9490
2	Australia	0.9191	0.9372	0.8519	0.8415
3	Heart	0.8626	0.8593	0.8633	0.8180
4	Teaching	0.6484	0.7978	0.7691	0.7572
5	Iono	0.8166	0.9105	0.8638	0.8502
6	Pima	0.7382	0.7771	0.741	0.7741
7	Bupa	0.5522	0.6573	0.7164	0.7012
8	Shuttle	0.9252	0.964	0.9817	0.9854
9	Parkinson	0.7844	0.8632	0.9349	0.9175
10	Titanic	0.8045	0.795	0.7703	0.7718
11	Sonar	0.8218	0.8476	0.6167	0.7833
12	Iris	0.9333	0.9511	0.9347	0.9472
13	Wine	0.914	0.9963	0.9636	0.9657
14	Balance	0.8855	0.929	0.9571	0.9277
15	Vehicle	0.7548	0.7177	0.7317	0.7425
16	Nursery	0.9351	0.9275	0.9028	0.9112
17	Zoo	0.9503	0.9402	0.9139	0.9414
18	Segment	0.7496	0.9356	0.8396	0.8375

19	Ecoli	0.7919	0.8686	0.8547	0.8391
20	Pendigit	0.9928	0.9944	0.9818	0.9785
		0.8311	0.8833	0.8429	0.8621

Bold values indicate the best value under same conditions.

Table 3. Average classification accuracy on 20 UCI data sets with polynomial kernel.

Index	Model / Data set	ker-NN	k -RV	RVM- Gauss	RVM- Bern
1	WBCD	0.9728	0.9695	0.7182	0.9222
2	Australia	0.7994	0.858	0.7826	0.7775
3	Heart	0.7782	0.8123	0.8001	0.7805
4	Teaching	0.5484	0.7978	0.7984	0.7428
5	Iono	0.7982	0.8194	0.8327	0.811
6	Pima	0.7993	0.839	0.7723	0.7711
7	Bupa	0.6926	0.6765	0.674	0.6625
8	Shuttle	0.9897	0.9947	0.9796	0.9805
9	Parkinson	0.9509	0.9542	0.9228	0.93
10	Titanic	0.7884	0.7909	0.8203	0.8217
11	Sonar	0.659	0.6286	0.7319	0.7183
12	Iris	0.9947	0.9984	0.8873	0.8755
13	Wine	0.9516	0.9585	0.9538	0.9412
14	Balance	0.8684	0.9075	0.8837	0.8618
15	Vehicle	0.8314	0.8210	0.8005	0.7932
16	Nursery	0.9635	0.9439	0.972	0.9538
17	Zoo	0.9403	0.9174	0.8329	0.7973
18	Segment	0.7496	0.7825	0.7327	0.7209
19	Ecoli	0.8861	0.8988	0.8996	0.8897
20	Pendigit	0.9810	0.9925	0.9705	0.9659
Average	-	0.8472	0.8641	0.8309	0.8308

Bold values indicate the best value under same conditions.

Following the results in Tables 2 and 3, k -RV is very competitive compared to other counterparts for both Gaussian and polynomial kernels. The second best winner is RVM-Bern. The proposed k -RV is also a clear winner compared to ker-NN. k -RV outperforms ker-NN on several UCI datasets, with 4% gap in average CA for Gaussian kernel and 1.7% gap in for polynomial kernel. This implies that sparsity plays an important role in data classification with nearest neighbor rules.

Tables 4 and 5 display the optimal number of RVs (# RV), the optimal width, the optimal $\Delta\alpha$ (delta) and the number of relevant attributes (#used) for Gaussian and polynomial kernels respectively. The main point to be mentioned, for all datasets, at least 95% of training vectors (#used) are pruned by k -RV while the performance of k -RV is still better than ker-NN.

Table 4. Number of used hidden nodes for several datasets (*Gaussian* hidden nodes)

Dataset	<i>k</i> -RV	Dataset	<i>k</i> -RV
	(# RV, width, delta, # used)		(# RV, width, delta, # used)
Wbcd	(6, 0.05 10, 0.012)	Iris	(1, 0.7, 0.1, 0.052)
Australia	(5, 0.4, 10, 0.035)	Wine	(2, 0.35, 5, 0.031)
Heart	(6, 5, 0.1, 0.12)	Balance	(1, 1, 5, 0.009)
Teaching	(6, 0.9, 0.1, 0.037)	Nursery	(41, 0.01, 1, 0.0032)
Iono	(1, 1, 5, 0.016)	Zoo	(6, 1, 1e-5, 0.06)
Pima	(8, 0.9, 5, 0.007)	Segment	(4, 0.5, 0.01, 0.04)
Bupa	(9, 0.95, 0.01, 0.026)	Ecoli	(5, 1, 1e-6, 0.017)
Shuttle	(1, 0.95, 5, 0.057)	Pendigit	(51, 0.1, 10, 0.0046)
Parkinson	(3, 0.75, 5, 0.017)	Vehicle	(2, 0.45, 1, 0.056)
Sonar	(6, 5, 0.1, 0.02)	Titanic	(7, 0.6, 5, 0.0025)

Table 5. Number of used hidden nodes for several datasets (*polynomial* hidden nodes)

Dataset	<i>k</i> -RV	Dataset	<i>k</i> -RV
	(# RV, width, delta, # used)		(# RV, width, delta, # used)
Wbcd	(3, 0.25, 1e-6, 0.024)	Iris	(1, 0.6, 1e-5, 0.038)
Australia	(7, 0.4, 0.01, 0.003)	Wine	(5, 0.9, 10, 0.019)
Heart	(7, 1, 0.001, 0.078)	Balance	(1, 0.7, 0.001, 0.0036)
Teaching	(6, 0.9, 0.1, 0.037)	Nursery	(14, 0.45, 1e-6, 0.001)
Iono	(11, 1, 1e-5, 0.003)	Zoo	(6, 1, 1e-5, 0.06)
Pima	(5, 0.75, 1e-5, 0.013)	Segment	(4, 0.5, 0.01, 0.04)
Bupa	(9, 0.5, 1, 0.006)	Ecoli	(5, 1, 1e-6, 0.017)
Shuttle	(2, 0.85, 1e-6, 0.066)	Pendigit	(44, 0.1, 10, 0.0045)
Parkinson	(5, 0.5, 1e-4, 0.006)	Vehicle	(3, 0.5, 1, 0.059)
Sonar	(1, 0.6, 1e-4, 0.005)	Titanic	(3, 0.8, 0.001, 0.001)

Fig. 3 displays the number of basis vectors and sparse basis vectors for ker-NN and *k*-RV respectively. Referring to Fig. 3, the number of vectors in ker-NN is nearly 100 times greater than the non-zero vectors of *k*-RV for all UCI datasets.

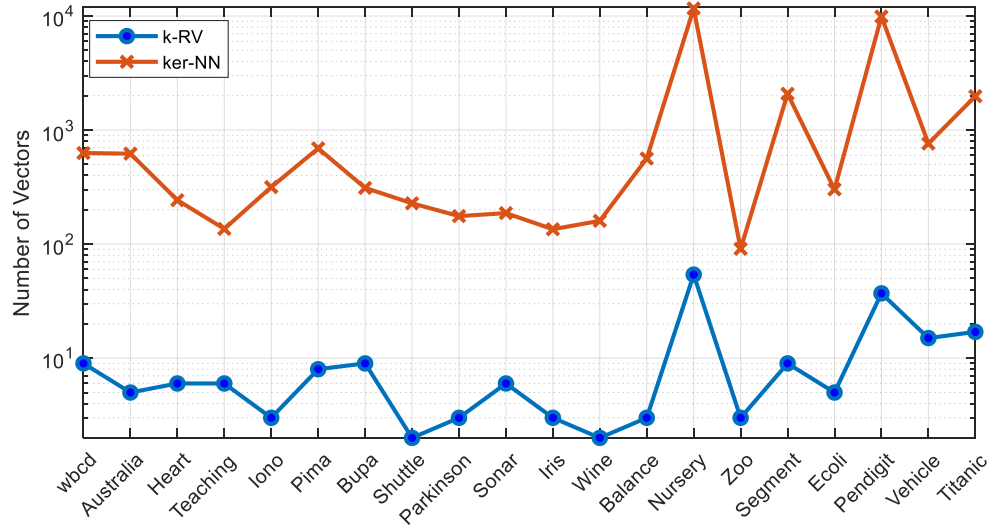


Fig. 3 Training vectors of ker-NN versus relevance vectors of k -RV. The y-axis is in log scale

Fig. 4 illustrates relevant attributes and their weight values for Iris dataset. Only those vectors with non-zero weights take a part in the classification of query instances. The weight values are distributed in the range of $[-1,1]$. Among 120 attributes of training data, only 8 attributes and their corresponding non-zero weights are used to find k relevance vectors through Eq. (8). This example emphasizes the ability of k -RV in significant sparsification of data while the CA is even better than a kernelized nearest neighbor rule that is not sparsed.

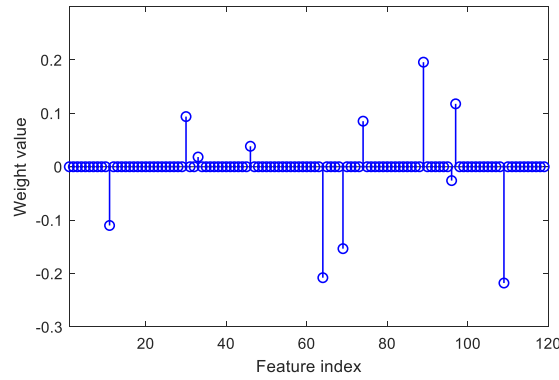


Fig. 3. Relevant attributes and their corresponding weight values

The k -RV and ker-NN models were run 10 times with 10-fold cross validation. Given 100 values of CAs, a statistical significance between k -RV and ker-NN based on a 95% confidence paired-t test is shown in Table 6. The hypothesis S with value '1' rejects the null hypothesis that the means of compared methods are equal, '0' otherwise.

Table. 6. 10 runs of 10-fold cross validation

Index	Model / Data set	k -RV	ker-NN	S
1	WBCD	0.9419	0.9267	0
2	Australia	0.9372	0.9191	0
3	Heart	0.8593	0.8626	0
4	Teaching	0.7978	0.6484	1
5	Iono	0.9105	0.8166	1
6	Pima	0.7771	0.7382	1
7	Bupa	0.6573	0.5522	1
8	Shuttle	0.964	0.9252	1
9	Parkinson	0.8632	0.7844	1
10	Titanic	0.795	0.8045	0
11	Sonar	0.8476	0.8218	0
12	Iris	0.9511	0.9333	0
13	Wine	0.9963	0.914	1
14	Balance	0.929	0.8855	1
15	Vehicle	0.7177	0.7548	0
16	Nursery	0.9275	0.9351	0
17	Zoo	0.9402	0.9503	0
18	Segment	0.9356	0.7496	1
19	Ecoli	0.8686	0.7919	1
20	Pendigit	0.9944	0.9928	0

Bold values indicate the best value under same conditions.

Referring to Table 6, the last column, the proposed k -RV is statistically significant compared to ker-NN on 10 out of 20 UCI datasets.

4.3 Computer Vision Data Experiments

Table 7 and Table 8 tabulate the performance of learners on two real-world datasets, GTSRB and MNIST, with Gaussian and polynomial kernels respectively.

Table 7. Classification accuracies and computed time on real-world datasets (*Gaussian* kernel)

Model/Data set	GTSRB			MNIST		
	Accuracy	Train time	Test time	Accuracy	Train Time	Test Time
RVM-GK	0.9406	30h 28min	27sec	0.9745	32h 22min	31sec
RVM-Bern	0.9339	29h 10min	29sec	0.9719	32h 7min	32sec
ker-NN	0.9217	4h 10min	1min 43sec	0.9606	5h 3min	2min 28sec
k -RV	0.9526	53h 11min	1min 14sec	0.9841	57h 20min	2min 7sec

Boldface indicates the highest accuracy among classifiers under same conditions.

Table 8. Classification accuracies and computed time on real-world datasets (*polynomial* kernel)

Model/Data set	GTSRB			MNIST		
	Accuracy	Train time	Test time	Accuracy	Train Time	Test Time
RVM-Gauss	0.9406	30h 20min	27sec	0.9745	34h 9min	31sec
RVM-Bern	0.9339	29h 36min	29sec	0.9719	31h 24min	32sec
ker-NN	0.9217	4h 10min	1min 43sec	0.9606	5h 14min	2min 2sec
<i>k</i> -RV	0.9526	53h 17min	1min 8sec	0.9841	57h 5min	1min 51sec

Boldface indicates the highest accuracy among classifiers under same conditions.

Comparing results in Tables 7 and 8, *k*-RV significantly outperforms ker-NN for both GTSRB and MNIST datasets, with polynomial and Gaussian kernel functions respectively. ker-NN is the fastest algorithm among all learners, however, it has the worst CA. *k*-RV with Gaussian kernel gains highest test accuracies 0.9526 and 0.9841 on GTSRB and MNIST respectively. The gap in test accuracies between *k*-RV and second best winner, RVM-Gauss, is nearly 1%. However, this small gap means *k*-RV can correctly classify nearly 120 test images more than RVM-Gauss since GTSRB has more than 12,000 test images. But, the test time of RVM-Gauss is much better than our proposed *k*-RV since the test prediction in *k*-RV delays for every test instance as *k*-RV is a memory based learner and regionally classifies each test instance. Moreover, referring to Eq. (6), RVM requires the inversion of covariance matrix that is timely. The test time of *k*-RV is better than ker-NN since *k*-RV uses sparsed weights and attributes to classify test instances while ker-NN is a dense learner and uses all weights and attributes.

5. Discussion

One aspect of our modelling to be mentioned is, RVM has poor predictions for those query instances are far away from the RVs. In [37], the source of problem is attributed to the degeneracy of covariance function. Intuitively, the fewer RVs, more probably the lower is the performance. Thus, the early stopping of RVM helps to have more RVs, hence better performance. we adjust the $\Delta\alpha$ and width of *Gaussian* kernel of basis functions to resolve the issue of the degeneracy of covariance function in RVM. Fig. 10 displays the plot of RVM application on Ripley’s synthetic data. As it can be seen, adjustment of $\Delta\alpha$ generates more RVs. Distance is an important feature of our *k*-RV for accurate estimation of the target value and with generating more RVs, the input space has adjacent RVs for every query instance.

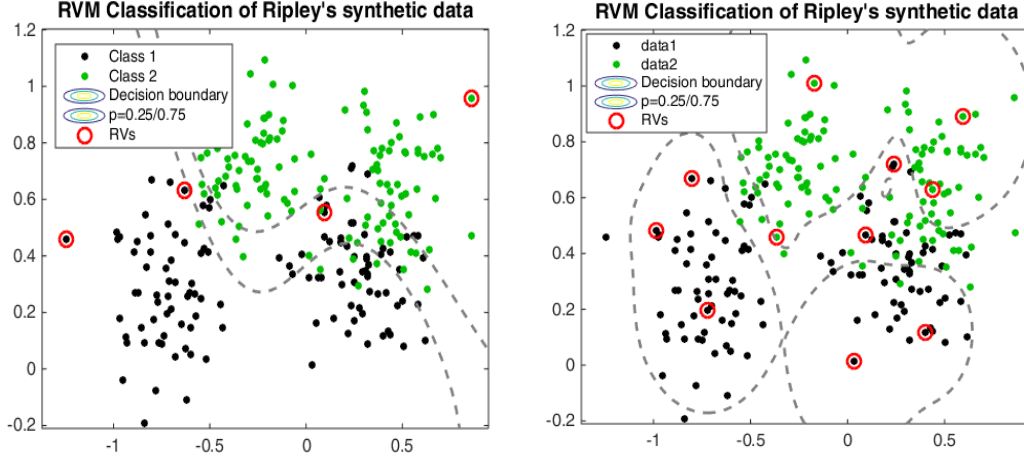


Fig. 5. The newly introduced parameter generates different number of RVs. Left: Relevance vectors of k -RV with $\Delta\alpha = 0.001$, Right: Relevance vectors of k -RV with $\Delta\alpha = 0.01$.

To verify the effectiveness of the new parameter $\Delta\alpha$, we also compare RVM-Gauss when α is fixed with RVM-Gauss when α is adjusted (RVM⁺-GK). Table 9 shows this comparison.

Table 9. Average classification accuracy of RVM-GK versus RVM⁺-GK

Index	Model / Data set	RVM-Gauss	RVs	RVM ⁺ -Gauss	RV ⁺ s
1	WBCD	0.6964	7	0.8875	19
2	Australia	0.8519	4	0.8827	9
3	Heart	0.8633	8	0.8694	18
4	Teaching	0.7691	9	0.7980	22
5	Iono	0.8638	3	0.8953	8
6	Pima	0.741	6	0.8125	14
7	Bupa	0.7164	10	0.7449	20
8	Shuttle	0.9817	4	0.9822	13
9	Parkinson	0.9349	5	0.9579	14
10	Titanic	0.7703	5	0.7993	11
11	Sonar	0.6167	5	0.6645	19
12	Iris	0.9347	3	0.9490	14
13	Wine	0.9636	3	0.9632	11
14	Balance	0.9571	7	0.9574	26
15	Vehicle	0.7317	8	0.7433	14
16	Nursery	0.9028	40	0.9155	48
17	Zoo	0.9139	7	0.9373	11
18	Segment	0.8396	5	0.8522	42
19	Ecoli	0.8547	4	0.8522	14
20	Pendigit	0.9818	54	0.9836	95
Average	-	0.8429	9.85	0.8727	22.1

Referring to table 9, RVM⁺-Gauss has better CA than RVM-Gauss on most datasets. To justify this better performance, we observe that the number of RV⁺s is greater than the number of RVs for every dataset. This implies that the traditional RVM prunes the datasets excessively, resulting in the degeneracy of covariance function [37]. The degeneracy means that the rank of the

kernel matrix is equal to the number of RVs. Thus, the matrix is very low rank and ill-conditioned. The new parameter $\Delta\alpha$, plays as a role of early stopping. This parameter does not allow RVM to prune data undesirably. Hence, more RVs are preserved and the rank increases. Fig. 5 also shows how adjusting the new parameter $\Delta\alpha$ generates more RVs.

6. Conclusion

In this study, we linked two different learning approaches, memory-based learning and statistical learning. We showed that only very few relevant attributes and their corresponding weights are enough to improve the classification accuracy of the k -NN. Experiments conducted on several datasets with two different types of kernel showed the advantage of the proposed k -RV over a few state-of-the-arts. The new parameter that controls the stopping condition of RVM helped to produce more RVs and heal the degeneracy of covariance function in RVM. Thus, higher classification accuracy obtained by k -RV. Future research direction is conducted on improving the speed of the proposed algorithm with graphical processing unit (GPU) since k -RV has slow training time.

Author Contribution

Peyman Hosseinzadeh Kassani and Sara Hosseinzadeh Kassani are co-first authors and contributed equally to this work.

References:

1. Kassani S. and P. Kassani, *A Comparative Study of Deep Learning Architectures on Melanoma Detection*. Tissue and Cell, 2019. **58**: p. 76-83.
2. Jang, S.-I., et al., *Online Heterogeneous Face Recognition Based on Total-Error-Rate Minimization*. IEEE Transactions on Systems, Man, and Cybernetics: Systems, 2018: p. 1-14.
3. Kassani, S., P. Kassani, and S.E. Najafi., *Introducing a hybrid model of DEA and data mining in evaluating efficiency. Case study: Bank Branches*. Academic Journal Of Research In Economics And Management, 2015.
4. Stallkamp, J., et al. *The German traffic sign recognition benchmark: a multi-class classification competition*. in *Proc. Int. Joint Conf. Neural Networks*. 2011.
5. Tu, E., et al., *A graph-based semi-supervised k nearest-neighbor method for nonlinear manifold distributed data classification*. Information Sciences, 2016. **367–368**: p. 673-688.
6. Karthick Ganesan, H.R., *Performance Analysis of KNN Classifier with Various Distance Metrics Method for MRI Images*, in *Part of the Advances in Intelligent Systems and Computing book series (AISC, volume 900)*. 2012. p. 673-682.
7. Bhaduri, S., et al. *Classification of lower limb motor imagery using K Nearest Neighbor and Naïve-Bayesian classifier*. in *3rd International Conference on Recent Advances in Information Technology (RAIT)*. 2016. Dhanbad, India.

8. Duda, R.O., Hart, P.E., , *Pattern classification and scene analysis*. 1973, New York: John Wiley and Sons,.
9. Cortes, C. and V. Vapnik, *Support-Vector Networks*. Machine Learning,, 1995. **20**: p. 273-297.
10. Quinlan, J.R., *Simplifying decision trees*. International Journal of Man-Machine Studies, 1987. **27** (3).
11. Cover, T. and Hart P.E., *Nearest neighbor pattern classification*. IEEE Transaction on Information Theory, 1967. **13**: p. 21-27.
12. Wu, X., et al., *Top 10 algorithms in data mining*. Knowledge and Information Systems. **14**(1): p. 1–37.
13. Lavrač, N., *Selected techniques for data mining in medicine*. Artificial Intelligence in Medicine, 1999. **16**(1): p. 3-23.
14. Gopinath, B. and N. Shanthi, *Development of an Automated Medical Diagnosis System for Classifying Thyroid Tumor Cells using Multiple Classifier Fusion*. Technology in Cancer Research and Treatment 2015. **14**: p. 653-662.
15. Saraiva, R., et al., *Early diagnosis of gastrointestinal cancer by using case-based and rule-based reasoning*. Expert Systems with Applications, 2016. **61**: p. 192-202.
16. Lin, W.C., S.W. Ke, and H.F. Tsai, *CANN: An intrusion detection system based on combining cluster centers and nearest neighbors*. Knowledge-Based Systems, 2015. **78**: p. 13-21.
17. Serpen, G. and E. Aghaei, *Host-based misuse intrusion detection using PCA feature extraction and kNN classification algorithms*. Intelligent Data Analysis, 2018. **22**(5): p. 1101-1114.
18. Xia, M., et al., *A hybrid method based on extreme learning machine and k-nearest neighbor for cloud classification of ground-based visible cloud image*. Neurocomputing, 2015. **160**: p. 238-249.
19. Maillou, J., et al., *kNN-IS: An Iterative Spark-based design of the k-Nearest Neighbors classifier for big data*. Knowledge-Based Systems, 2017. **117**: p. 3-15.
20. Kassani P, Hyun J, and Kim E. *Proposing a GPU based modified fuzzy nearest neighbor rule for traffic sign detection*. in *15th International Conference on Control, Automation and Systems* 2015 IEEE.
21. Jo, T. *Using K Nearest Neighbors for text segmentation with feature similarity*. in *International Conference on Communication, Control, Computing and Electronics Engineering (ICCCCEE)*. 2017 Khartoum, Sudan: IEEE.
22. Surlakar, P., S. Araujo, and K.M. Sundaram. *Comparative Analysis of K-Means and K-Nearest Neighbor Image Segmentation Techniques*. in *IEEE 6th International Conference on Advanced Computing (IACC)*. 2016. Bhimavaram, India: IEEE.
23. López, J. and S. Maldonado, *Redefining nearest neighbor classification in high-dimensional settings*. Pattern Recognition Letters, 2018. **110**: p. 36-43.
24. Wangmeng Zuo, David Zhang, and Kuanquan Wang, *On kernel difference-weighted k-nearest neighbor classification*. Pattern Analysis Applications, , 2008. **11**: p. 247–257.
25. Ichiro Takeuchi and Masashi Sugiyama. *Target Neighbor Consistent Feature Weighting for Nearest Neighbor Classification*. in *Advances in Neural Information Processing Systems*. 2011.
26. Jahromi, M.Z., E. Parvinnia, and R. John, *A method of learning weighted similarity function to improve the performance of nearest neighbor*., Information Sciences,, 2009. **17**: p. 2964–2973.
27. Chen, L. and G. Guo, *Nearest neighbor classification of categorical data by attributes weighting*. Expert Systems with Applications, 2015. **42**(6): p. 3142-3149.
28. Tutza, G. and S. Ramzan, *Improved methods for the imputation of missing data by nearest neighbor methods*. Computational Statistics & Data Analysis 2015. **90**: p. 84-99.
29. Nitish Srivastava, et al., *Dropout: A Simple Way to Prevent Neural Networks from Overfitting*. Journal of Machine Learning Research, 2014. **15**: p. 1929-1958.
30. Lorenzo Rosasco, et al., *Nonparametric Sparsity and Regularization*. Journal of Machine Learning Research, 2013. **14**: p. 1665-1714.
31. M. E. Tipping, *Sparse Bayesian Learning and the Relevance Vector Machine*. Journal of Machine Learning Research, 2001. **1**: p. 211-244.
32. Jiahua Luo, Chi-Man Vong, and P.-K. Wong, *Sparse Bayesian Extreme Learning Machine for Multi-classification*. IEEE transactions on neural networks and learning systems, 2014. **25**(4): p. 836-843.
33. Huang, G.B., Q.U. Zhu, and C. Siew, *Extreme learning machine: Theory and applications*. Neurocomputing, 2006. **70**(1-3): p. 489-501.
34. Kassani, P.H. and A.B.J. Teoh, *A new sparse model for traffic sign classification using soft histogram of oriented gradients*. Applied Soft Computing, 2017. **52**: p. 231-246.
35. Toh, K.A., Q.L. Tran, and D. Srinivasan, *Benchmarking a reduced multivariate polynomial pattern classifier*, . IEEE Transactions on Pattern Analysis and Machine Intelligence, 2004. **26**(6).

36. Rismanchian, F. and K. Rahimian, *Proposing a Localized Relevance Vector Machine for Pattern Classification*. <https://arxiv.org/abs/1904.03688>.
37. Rasmussen, C.E. and J. Quiñero-Candela. *Healing the Relevance Vector Machine through Augmentation*. in *Proceedings of the 22nd International Conference on Machine Learning*. 2005.
38. Tipping, M.E., *Sparse Bayesian Learning and the Relevance Vector Machine*. Journal of Machine Learning Research, 2001. **1**: p. 211-244.
39. Cortes, C.V., V., *Support-vector networks*. Machine Learning, 1995. **20**(3): p. 273–297.
40. MacKay, J.C., *The evidence framework applied to classification networks*. Neural Comput., , 1992. **4**(5): p. 720-736.
41. Lecun, Y., et al., *Gradient-based learning applied to document recognition*. Proceedings of the IEEE., 1998. **86**(11): p. 2278-2324.
42. Dalal, N. and B. Triggs. *Histograms of oriented gradients for human detection*. in *IEEE Computer Society Conference on Computer Vision and Pattern Recognition (CVPR'05)*. 2005. San Diego, CA, USA,: IEEE.